Scalp Electrode Impedance, Infection Risk, and EEG Data Quality

Article *in* Clinical Neurophysiology · April 2001

DOI: 10.1016/S1388-2457(00)00533-2 · Source: PubMed

4 authors, including:

Thomas C Ferree
NeuroMetrix, Inc.
45 PUBLICATIONS **1,549** CITATIONS

SEE PROFILE

Phan Luu
University of Oregon
66 PUBLICATIONS **6,058** CITATIONS

SEE PROFILE

Don M Tucker
University of Oregon
290 PUBLICATIONS **12,695** CITATIONS

SEE PROFILE

ELSEVIER

Clinical Neurophysiology 112 (2001) 536–544

www.elsevier.com/locate/clinph

Scalp electrode impedance, infection risk, and EEG data quality

Thomas C. Ferree[a,b,*], Phan Luu[a,c], Gerald S. Russell[a,d], Don M. Tucker[a,c]

[a]*Electrical Geodesics, Inc., Riverfront Research Park, 1850 Millrace Dr., Eugene, OR 97403, USA*
[b]*Computational Science Institute, University of Oregon, Eugene, OR 97403, USA*
[c]*Department of Psychology, University of Oregon, Eugene, OR 97403, USA*
[d]*Regena Software, 12427 Carmel Cape, San Diego, CA 92130, USA*

Accepted 17 November 2000

Abstract

Objectives: Breaking the skin when applying scalp electroencephalographic (EEG) electrodes creates the risk of infection from blood-born pathogens such as HIV, Hepatitis-C, and Creutzfeldt–Jacob Disease. Modern engineering principles suggest that excellent EEG signals can be collected with high scalp impedance (≈40 kΩ) without scalp abrasion. The present study was designed to evaluate the effect of electrode-scalp impedance on EEG data quality.

Methods: The first section of the paper reviews electrophysiological recording with modern high input-impedance differential amplifiers and subject isolation, and explains how scalp-electrode impedance influences EEG signal amplitude and power line noise. The second section of the paper presents an experimental study of EEG data quality as a function of scalp-electrode impedance for the standard frequency bands in EEG and event-related potential (ERP) recordings and for 60 Hz noise.

Results: There was no significant amplitude change in any EEG frequency bands as scalp-electrode impedance increased from less than 10 kΩ (abraded skin) to 40 kΩ (intact skin). 60 Hz was nearly independent of impedance mismatch, suggesting that capacitively coupled noise appearing differentially across mismatched electrode impedances did not contribute substantially to the observed 60 Hz noise levels.

Conclusions: With modern high input-impedance amplifiers and accurate digital filters for power line noise, high-quality EEG can be recorded without skin abrasion.

Keywords: Electroencephalography; Scalp abrasion; Infection risk; Electrode impedance; Signal quality; 60 Hz Noise

1. Introduction

Before laboratory computers, the quality of the EEG record was dependent on the signal recorded on paper. Noise from power lines (50 or 60 Hz) could not be separated once it was introduced, and the required procedure was to abrade the skin to achieve a scalp-electrode impedance of less than 5 kΩ. To achieve such impedance levels, skin abrasion is required. Abrasion removes the surface epidermal layer, which has higher impedance than the underlying tissue.

1.1. Electrode infection risk

The primary concern with breaking the skin is infection risk. Once the scalp is abraded, the electrodes or their attachments are likely to contact blood products (Putnam et al., 1992). Infection with a blood-borne pathogen, such as human immunodeficiency virus (HIV), hepatitis C virus (HCV), or Creutzfeldt–Jacob Disease (CJD), may be unsymptomatic for many years before manifesting as a terminal disease. The United States Center for Disease Control (www.cdc.gov) has issued guidelines for the prevention of blood-born pathogens through disinfection and sterilization of reusable instruments (CDC, 1991, 2000):

1. instruments that touch intact skin are non-critical and should be disinfected with low-level or intermediate disinfection;
2. instruments that touch mucous membranes but will not touch bone or penetrate tissue are semi-critical and should be subject to high-level disinfection if they cannot be sterilized;
3. instruments that touch bone or penetrate tissue are critical and must be sterilized

Remarkably, sterilization is not adequate to destroy the prion pathogen of CJD (American Electroencephalographic Society, 1994). After intracranial EEG electrodes had accidentally caused transmission of CJD from a demented

* Corresponding author. Tel.: +1-541-687-7962; fax: +1-541-687-7963.
E-mail address: tom@cortex.egi.rrp.net (T.C. Ferree).

1388-2457/01/$ - see front matter CLINPH 2000102
PII: S1388-2457(00)00533-2

patient to two younger epileptic patients, the electrodes were implanted in the brain of a chimpanzee. The animal developed CJD within 18 months (Gibbs et al., 1994). To date, there have been no documented cases of transmission of CJD through the use of scalp EEG electrodes.

When breaking the skin through scalp abrasion, EEG electrodes may come into contact with blood products, and it is therefore not adequate to disinfect them, as has been recommended by Putnam et al. (1992). Rather, to meet CDC guidelines, electrodes that contact broken skin must be sterilized. Current research guidelines recommend not only scalp abrasion but puncturing the skin under each electrode with a surgical lance in order to reduce skin potentials (Picton et al., 2000). Using a sterile lance is ineffective if the punctured skin is then placed into contact with a non-sterile electrode. In most clinical EEG laboratories, EEG electrodes are disinfected before use on new patients. Whereas disinfection would meet CDC guidelines when electrodes are used on intact skin, sterilization should be required when electrodes contact blood products, as is possible with scalp abrasion.

1.2. Spatial sampling, application speed, and subject comfort

There are 3 additional drawbacks to scalp abrasion and skin puncturing. Modern EEG systems are able to record from 128 or 256 scalp sites. Lesioning each site individually may become painful, and it is not uncommon for subjects to refuse EEG recording based upon discomfort. Without recording from sufficient scalp sites, the recording of the scalp potential misses meaningful spatial variations. Similar to what occurs in the time domain with inadequate spatial sampling, this shows up as aliasing in the spatial Fourier domain (Srinivasan et al., 1998). Furthermore, individual site preparation precludes rapid application of an EEG sensor (electrode) array in emergency settings and field hospitals. Though certainly important, these factors are secondary in relation to the risk of infection by blood-born pathogens. The following review of modern engineering principles explains why scalp abrasion is no longer necessary.

1.3. EEG recording with high input-impedance differential amplifiers

In EEG recordings, electric potential or voltage is measured on the scalp surface, and used to detect and localize the activity of the brain. The physical definition of electric potential requires that it always be measured as a difference between two sites. This is accomplished with differential amplifiers. Huhta and Webster (1973) presented an essentially complete analysis of signal loss and 60 Hz noise in electrocardiographic (ECG) recordings using differential amplifiers. Our analysis extends theirs in two main ways to make it relevant to modern EEG.

First, Huhta and Webster assumed that the subject was connected to earth ground. This simplification reduces the number of variables in the calculations, but it is no longer appropriate. Grounding the subject is unsafe because it increases the risk of electric shock. Modern safety regulations require that the subject must be isolated from ground so that contact with an electric source would not result in the subject creating a path to ground. Furthermore, grounding also allows more 60 Hz noise to enter the measurements. Modern amplifiers use an 'isolated common' electrode which is electrically isolated from the ground of the power supply. In this configuration, the potential of both measurement and reference leads are measured relative to this common electrode and only their difference is amplified. Since the subject is only capacitively coupled to ground, the 60 Hz noise due to electric fields is greatly reduced.

Second, Huhta and Webster assumed the ground electrode was connected to the subject's foot, at maximal distance from the recording and reference electrodes which were located on the torso for cardiac recording. This supports the assumption that the ground electrode is electrically quiet, which is convenient for interpreting the resulting signals. In EEG systems, however, both the reference and common electrodes are usually located on the head in order to minimize 60 Hz common-mode noise sources, as well as physiological noise from cardiac sources. In general, non-zero sources of potential difference will exist between each electrode and the common, as well as between the recording and reference electrodes.

Fig. 1 shows an idealized circuit diagram for measuring EEG data on the head using a differential amplifier with an isolated common lead. Z_1 and Z_2 represent the scalp-electrode impedances for recording and reference electrodes, respectively, and Z_c represents the scalp-electrode impedance for the common electrode. Z_{in1} and Z_{in2} represent the amplifier input impedances for recording and reference electrodes, and Z_d represents the amplifier differential input impedance. E_{12}, E_{1c} and E_{2c} represent bioelectric sources

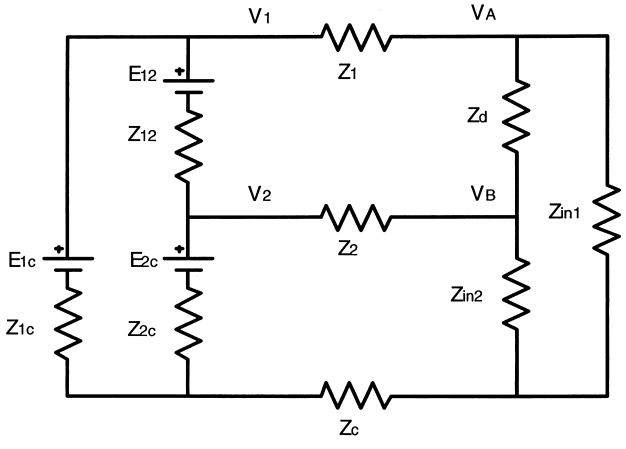

Fig. 1. Idealized circuit diagram for understanding the relationship between scalp-electrode impedance and amplifier input impedance.

located between the designated electrodes. In reality, brain sources are not DC but are oscillatory and broad-banded. Since the physics of volume conduction in biological tissue is quasi-static, however, at each time point these AC sources may be considered as effective DC sources (Nunez, 1981). Z_{12}, Z_{1c} and Z_{2c} represent the bulk impedance of the head tissue between the designated electrodes. V_1 and V_2 are the scalp potentials just below the scalp-electrode interface, whose difference we are trying to measure, and $(V_A - V_B)$ is the potential difference measured by the amplifier.

Our first objective is to quantify how $(V_A - V_B)$ differs from $(V_1 - V_2)$ as a function of scalp electrode and amplifier input impedances. These potentials differ because of current flow into the amplifiers and because of external electric and magnetic fields coupling to the electrode leads and body. As shown below, to a first approximation this signal loss depends on the average impedance of measurement and reference electrodes relative to the amplifier input impedance, whereas 60 Hz electric noise depends upon electrode impedance mismatches, and 60 Hz magnetic noise is independent of electrode impedance. For normally distributed data, the absolute impedances and their possible mismatches will be related because a distribution of higher impedance values will also tend to have higher mismatches, e.g. a set of scalp electrodes with 1–5 kΩ impedances will have mismatches of at most about 4 kΩ, while a set with 10–50 kΩ impedances will have mismatches of at most about 40 kΩ. Note also that as sponge electrodes dry the impedances drift up to 50–100 kΩ, but if all the electrodes dry together then the mismatches remain at most about 50 kΩ.

1.4. Signal amplitude attenuation

Whenever electric current flows through an impedance there is an associated potential drop. At the scalp-electrode interface, a higher impedance results in a higher voltage drop and some attenuation of signal amplitude. This is a well-known problem which has a standard remedy. By designing amplifiers which have input impedances much higher than the scalp-electrode impedances, the current flow is made low enough that the corresponding potential drop is negligible.

Using Ohm's law and current conservation on the circuit in Fig. 1 leads to 9 linear equations for the 9 unknown currents in each branch of the circuit. Solving these equations simultaneously leads to an exact expression for the measured difference $(V_A - V_B)$ in terms of brain sources. To simplify the result, we made following assumptions: First, we assumed that Z_{12}, Z_{1c} and Z_{2c} are small, which is reasonable in comparison to the scalp-electrode impedances and amplifier input impedances. (Numerical estimates of human whole-head impedances are given below.) Second, we assumed that $Z_d \gg Z_{in}$, neglecting the differential amplifier impedance. Third, we assumed that the amplifier input impedances were balanced, i.e. $Z_{in1} = Z_{in2}$, in order to stay focussed on the role of scalp-electrode impedances rather than amplifier imperfections. We then defined the differential-mode signal $V_D = (V_1 - V_2)/2$. and the common-mode signal $V_C = (V_1 + V_2)/2$, and expressed $(V_A - V_B)$ in terms of them. Working within our basic assumption that the amplifier input impedance is large compared to the scalp-electrode impedances, we expanded $(V_A - V_B)$ in a Taylor series in the quantity $1/Z_{in}$ and kept only linear terms. This results in the following expression for the measured potential difference

$$(V_A - V_B) = V_D\left(2 - \frac{Z_2 + Z_1}{Z_{in}}\right) + V_C\left(\frac{Z_2 - Z_1}{Z_{in}}\right) + O\left(\frac{1}{Z_{in}}\right)^2$$

The left hand side is the potential difference across the two leads as measured by the differential amplifier. The first term on the right hand side is the differential-mode signal V_D multiplied by a factor which indicates attenuation of that signal as a function of the average scalp-electrode impedance and amplifier input impedance. The second term on the right hand side is the common-mode signal, originating mainly from 60 Hz ambient noise, multiplied by a factor which depends on the impedance mismatch. We will return to the second term below. The first term can be used to provide numerical estimates of signal loss for various amplifier and electrode systems.

Many modern EEG amplifiers have input impedances consisting of a resistive component on the order of 200 MΩ. In our amplifier, this resistance is in parallel with a capacitive component on the order of 10 pF, providing a reactance of 265 MΩ at 60 Hz. To make numerical estimates, we assumed $Z_{in} \approx 200$ MΩ. Assuming that with scalp abrasion Z_1 and Z_2 are at most 5 kΩ, the maximum signal loss is 0.0025%, which is completely negligible. Assuming that without scalp abrasion Z_1 and Z_2 are at most 50 kΩ, their maximum signal loss is 0.025%, which is an order of magnitude larger but still completely negligible. Some older differential amplifier systems have input impedances of closer to 10 MΩ. Even in this case, assuming electrode impedances up to 50 kΩ, the maximum signal loss is 0.5%, which may still be negligible for most purposes. Thus signal attenuation is expected to be insignificant without scalp abrasion, even when modestly high input-impedance amplifiers are used.

1.5. Environmental sources of 60 Hz noise

AC devices in the recording environment introduce 60 Hz noise into the data. This occurs because electric and magnetic fields incident on the electrode leads and body generate potentials which add linearly to the signal. Huhta and Webster (1973) have considered the sources and effects of 60 Hz noise when using differential amplifiers for ECG, assuming that the subject was connected to true ground. This simplifies the calculations, but increases the risk of electric shock and increases the amount of 60 Hz noise contaminating the recording. The standard practice now is to measure all potentials relative to a dedicated common

electrode which is electrically isolated from ground. This improves subject safety and reduces 60 Hz noise. The following discussion derives how 60 Hz noise amplitude may be expected to vary as a function of circuit parameters, when using a differential amplifier and an isolated common electrode located on the head.

1.6. Magnetic induction

Alternating currents in the recording environment produce time varying magnetic fields. By Faraday's law, a conducting loop will experience an induced potential if oriented properly with respect to the field. For a simple loop of conducting wire, the potential induced across the end of the loop is equal to

$$V_M = 2\pi fAB$$

where $f = 60$ Hz, A is the loop area and B is the vector component of the 60 Hz magnetic field oriented perpendicular to the loop surface. The primary contribution to $(V_A - V_B)$ comes from the current loop formed by the measurement and reference electrode leads and partly the head. Yet with a common electrode, a potential difference can also be induced magnetically in the two other loops formed by the measurement and reference electrodes with the common electrode. Depending upon how the individual loops are oriented with respect to the field, these contributions may effectively add or cancel. In ECG, it is usually recommended that the leads be twisted near the chest before running to the amplifier, minimizing the loop area and reducing magnetic noise. In EEG, the leads are typically bundled near the head before running to the amplifier, and this was the case in our experiments.

The amplitude of the magnetic field B and induced potential V_M depends upon the recording environment. To estimate of the size of V_M in a typical recording environment, we first assumed a magnetic field value equal to that measured by Huhta and Webster (1973): $B = 0.32$ μWb/m^2. Taking the maximum effective loop area to be one-half the cross-sectional area of a human head with radius $r = 9.2$ cm gives $A \approx 133$ cm^2. This leads to $V_M \approx 1.6$ μV, which would be detectable by most EEG amplifiers. This estimate of the magnetic noise amplitude is consistent with the amount of 60 Hz noise seen in Figs. 4, 5 and 6, and supports the hypothesis that much of the noise in our recordings may have been due to magnetic fields. Using a simple loop of wire and the same amplifier system we measured similar 60 Hz potentials, and found that this increased by an order of magnitude when the loop was put near the isolation transformer.

1.7. Electric displacement currents

Background electric fields also produce 60 Hz noise in bioelectric recordings. This can occur by 3 similar mechanisms, in which the background electric field couples to the electrode leads, to the conductive volume of the subject, or to components of the amplifier system. In all cases, the 60 Hz potential relative to ground causes additional currents to flow to ground. We assume here that most electric displacement coupling occurs through the electrode leads. In this mechanism, even though the induced current is likely to be similar in the different leads, electrode impedance imbalances produce 60 Hz noise in the measured signal.

Fig. 2 shows a simplified circuit for understanding the origin of 60 Hz electric noise in EEG recordings by this mechanism. The scalp-electrode impedances and head tissue impedances are represented as in Fig. 1, but the EEG source elements are omitted to focus on the 60 Hz signal. The amplifier impedances are assumed to be infinite, which is justifiable here because the capacitive coupling of the body and amplifier to ground provide the primary current path for 60 Hz currents: We have determined experimentally that for our amplifier system $Z_g \approx 20$ MΩ at 60 Hz, an order of magnitude smaller than the amplifier input impedance Z_{in}. Coupling to the leads is introduced via capacitors, whose values (Z_{d1}, Z_{d2} and Z_{dc}) depend on the dielectric properties of the space between nearby AC devices and the EEG leads. Because these values are difficult to determine independently, following Huhta and Webster (1973), we express the capacitive coupling in terms of the current I_d induced in each lead. Because all 3 leads run together from the head to the amplifier and subjects are in the near field of the 60 Hz potential, the induced current is likely to be in phase and approximately equal across leads.

Using Ohm's law and current conservation on the circuit in Fig. 2 leads to the following equation for the amplitude of 60 Hz noise due to capacitive coupling

$$V_E = I_d(Z_2 - Z_1) + I_d\left(\frac{Z_{12}(Z_{1c} - Z_{2c})}{Z_{12} + Z_{1c} + Z_{2c}}\right)$$

Both terms are proportional to the induced current I_d. The first term depends only on the scalp-electrode impedance imbalance between measurement and reference electrodes,

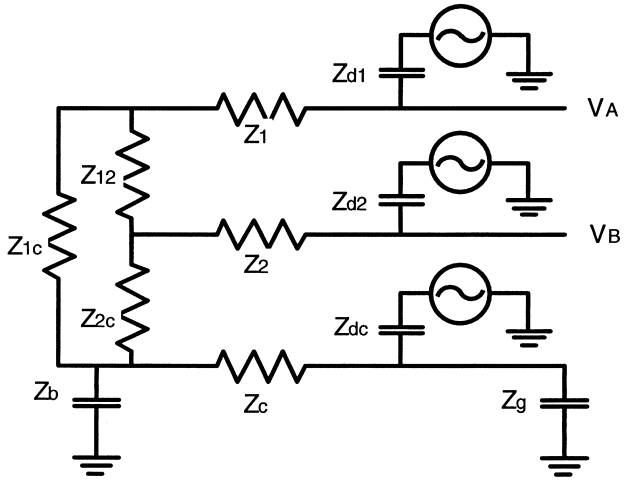

Fig. 2. Idealized circuit diagram showing capacitive coupling of 60 Hz electric noise into scalp electrode leads.

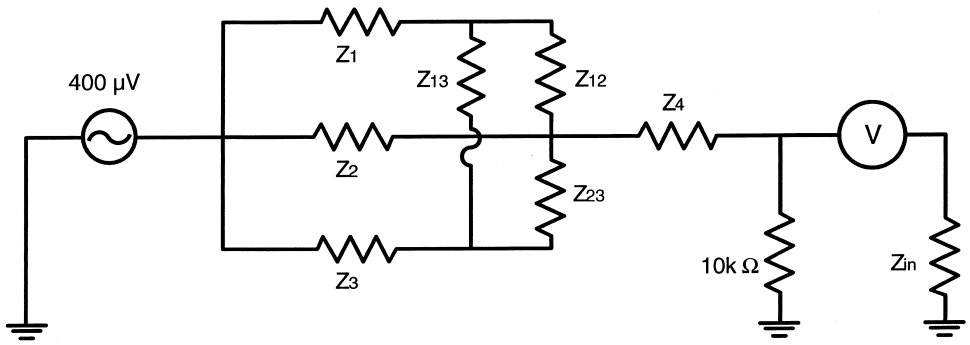

Fig. 3. Idealized circuit diagram for measuring scalp-electrode impedances.

while the second depends only on the impedances of the conducting head volume.

Huhta and Webster estimated $I_d = 6$ nA when grounding the subject in what they termed a poor recording environment with AC cords and equipment nearby. Using $I_d = 6$ nA and $(Z_2 - Z_1) = 40$ kΩ in the first term above leads to $V_E \approx 240$ μV, which is much larger than what is observed in our experiments. Displacement currents are substantially reduced, however, by the use of an isolated common electrode rather than a direct subject-ground connection. In Fig. 2, Z_{d1}, Z_{d2} and Z_{dc} represent distributed capacitances from diffuse 60 Hz noise sources to the two input cables and amplifier, respectively, while Z_b and Z_g represent distributed capacitances from the subject and amplifier to ground. Typically these impedances are all high and relatively symmetrical. Displacement currents are caused only by asymmetrical coupling into and out of the various components of the system. Assuming that all of the 60 Hz noise in Figs. 5 and 6 is due to this mechanism provides an upper limit on the electric displacement current in our recordings. Taking the maximum noise level to be 1 μV and the maximum impedance mismatch to be 40 kΩ implies that I_d may be at most 0.025 nA, more than two orders of magnitude below the estimate of Huhta and Webster (1973). This reduction is at least partly due to isolating the subject from earth ground. It may also be due in part to different noise characteristics of our recording environment.

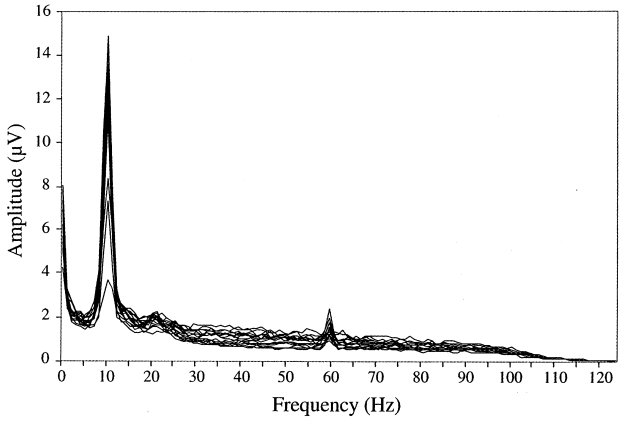

Fig. 4. EEG amplitude spectra (all conditions for one subject) showing alpha peak and 60 Hz noise.

Clearly, any amplifier system which does not use an isolated common return will be very sensitive to electrode impedance mismatch, due to high levels of I_d. However, while the isolated common grounding system reduces leakage currents I_d, the unfortunate impact is that high levels of capacitively coupled noise may appear on the isolated common potential relative to ground. In ideal amplifiers this noise is rejected perfectly, as the amplifier responds only to the differential input signal $(V_A - V_B)$. In real amplifiers, however, there is always some measurable response to noise driving the isolated common potential relative to ground. An amplifier's ability to reject this kind of noise is called its isolation mode rejection ratio (IMRR). Amplifier response to isolation mode noise is largely independent of electrode impedance mismatch, and is a possible source of the 60 Hz noise observed in our experiments.

The second term in the above equation may explain why in some experiments there tends to be more 60 Hz noise when the measurement electrode is located near the common electrode, a phenomenon well-known to EEG researchers. The second term is largest when Z_{1c} is very different from Z_{2c}, and vanishes when Z_{1c} is equal to Z_{2c}. The head impedances Z_{ij}, which appear in the second term, are difficult to measure independently in living humans, but can be estimated using computer simulations of volume conduction through biological tissue and assuming standard radii and conductivity values for the human brain, CSF, skull and scalp (Rush and Driscoll, 1969; Ferree et al., 2000). We have done this in computer simulation by injecting current through a pair of electrodes and calculating the potentials at the underlying scalp locations. We assumed the electrodes to be 1 cm in diameter, and the injected current to be distributed uniformly over its surface area. (In reality, most current flows along the outer edge of the electrode (Wiley and Webster, 1982), but this is ignored in our estimates.) Within these approximations, we find head impedance values ranging 300–500 Ω, depending upon the distance between the injection electrodes and the choice of skull conductivity. The location of the reference and common electrodes are usually fixed. Assuming

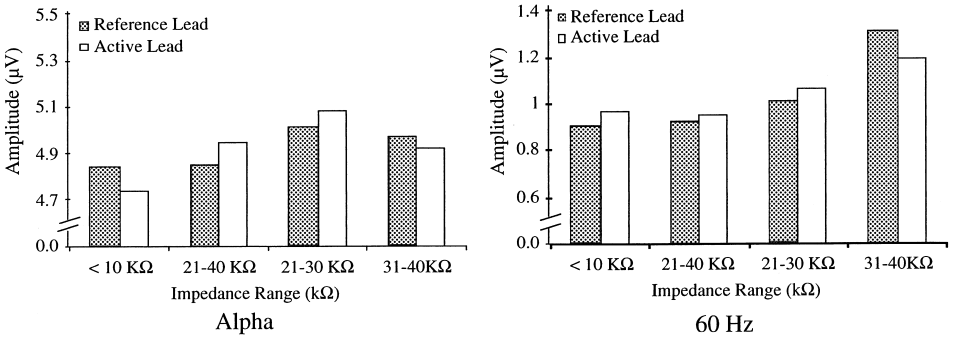

Fig. 5. Signal amplitude (μV) as a function of reference and measurement electrode impedance range (kΩ) for alpha and noise bands.

$Z_{1c} \approx Z_{12} \approx Z_{2c}$, as when the electrodes are evenly distributed over the head, this term makes no contribution. Assuming $Z_{1c} \approx 300\ \Omega$ and $Z_{12} \approx Z_{2c} \approx 500\ \Omega$, as when the measurement electrode is located near the common electrode, and assuming the induced current $I_d \approx 0.025$ nA, we find $V_E \approx 1.9$ nV for the second term, which is not reliably measurable with any EEG system. Thus 60 Hz noise near the nasion may arise by this mechanism alone only if the induced current I_d is substantially higher.

2. Methods and materials

2.1. Measurement of scalp-electrode impedance

To quantify the dependence of EEG signal quality on scalp-electrode impedance, we need to be able to measure scalp-electrode impedances accurately. Ideally this would be done by passing a known current across the scalp-electrode interface, and measuring the potential difference between points just above the electrode and just below the scalp. Since making an independent measurement of the potential just below the scalp surface is impractical, an approximate method is required. Fig. 3 shows a circuit diagram for this purpose. Only 4 electrodes are shown, when in practice there would be 20, 130, etc. Z_1 through Z_4 represent the 4 scalp-electrode impedances in a configuration for measuring impedance Z_4. The head impedances are shown, but are omitted from the calculations below since they are small compared to the scalp-electrode impedances. This particular approximation is more valid without scalp abrasion.

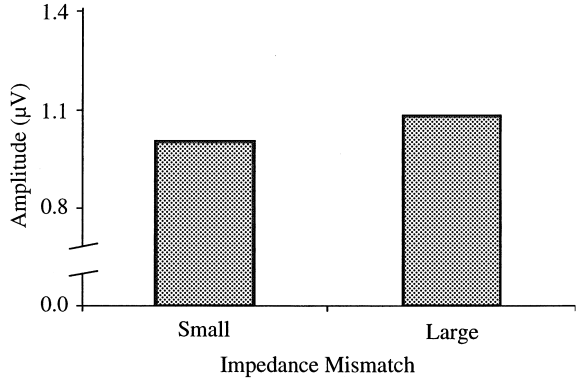

Fig. 6. Signal amplitude (μV) in the 60 Hz noise band. for small (<10 kΩ) and large (>10 kΩ) impedance mismatch conditions.

A simple method for measuring the scalp-electrode impedance Z_4 is based on the fact that, when K similar resistors ($Z_1 \approx Z_2 \approx Z_K$) are connected in parallel, they have an effective resistance which is smaller according to the formula

$$\frac{1}{Z_{\text{eff}}} = \frac{1}{Z_1} + \frac{1}{Z_2} + \ldots\ldots + \frac{1}{Z_K} \approx \frac{K}{Z_1}$$

Thus by driving all but one of the electrodes to a known potential relative to ground (400 μV), the potential at the scalp will be very nearly equal to the known potential. For K sufficiently large, the error in such an approximation may be estimated by the addition of one term, or $1/K$. For a 128-channel amplifier, $K = 128 - 1$ and the error is approximately $1/(128 - 1)$ or 0.79%, and to a very good approximation it is as though the impedance Z_4 is connected directly the 400 μV source. The remaining circuit is a simple voltage divider, and by measuring the potential V the value of Z_4 is given by

$$Z_4 = \frac{10\ \text{k}\Omega\ (400\ \mu\text{V} - V)}{V}$$

The amplitude V must be determined from the oscillatory signal. This is reasonably straightforward, but takes some computer time for many channels. A faster but more approximate algorithm drives all but 6 electrodes at a time, and measures these 6 scalp-electrode impedances simultaneously. The error in this approximation is slightly larger. Since the same current flows in parallel through the 6 electrodes the error is roughly $6/(128 - 6)$ or 4.9%. This latter method was used to measure the scalp-electrode impedances in the present experiments.

2.2. Subjects

In order to provide experimental verification of the engineering principles discussed above, we collected EEG data from 10 normal subjects with and without scalp abrasion, with impedances that varied from <10 kΩ to 40 kΩ. We tested for loss of signal amplitude in 4 standard EEG frequency bands and at 60 Hz. All procedures were approved by the Electrical Geodesics, Inc. (EGI) Human Subjects Institutional Review Board.

2.3. EEG data collection

EEG data were recorded using the Geodesic Sensor Net (Tucker, 1993), which arranges 129 Ag/AgCl electrodes in a tension structure that insures the sensors are distributed evenly across the head surface. The EEG signals were amplified with a high input-impedance ($Z_{in} \approx 200$ MΩ) Net Amps dense-array amplifier (Electrical Geodesics, Inc.). The data were recorded with a 0.1 to 100 Hz analog band-pass filter and digitized at 250 samples/s with a 16-bit analog-to-digital converter. The data were collected with the common electrode located at the nasion and the reference electrode located at the vertex. The location of the measurement electrode was kept fixed to eliminate variances arising from the irregular spatial distribution of brain activity, and was located over the right occipital region because a strong biological signal (alpha) can be clearly identified.

The impedances of the reference and a single measurement channel were systematically and independently varied. When the Geodesic Sensor Net was applied with saline-sponge electrodes, the scalp-electrode impedances were approximately 40 kΩ. Lower impedance values were obtained by abrading the scalp with a ground glass preparation (Omni Prep, D.O. Weaver and Co.). Higher impedance values were obtained by wicking saline away from the sponge electrode (simulating the drying that occurs by evaporation over several hours of recording). Once the desired impedance levels for the reference and measurement electrodes were obtained, 2 min of eyes-closed, resting EEG were acquired for each subject.

2.4. Fourier spectral analysis

For each subject and condition, 5 10-s epochs of EEG were selected for their lack of obvious artifacts from within a two-minute recording. Each epoch was divided into 10 1-s segments, multiplied by a Hanning window to reduce bin-width artifacts, and Fourier transformed using a standard FFT algorithm. The resulting power spectra had 1 Hz frequency resolution, and were expressed as frequency-domain spectral amplitudes by taking the modulus of the appropriate Fourier coefficients. The amplitudes were normalized so that an integer-frequency sine wave with a 1 μV peak amplitude in the time domain would result in a 1 μV spectral amplitude in the frequency domain. In the end, the amplitude spectra for all fifty 1-s epochs were averaged to provide a stable measure of EEG activity for that condition. We defined delta (1–3 Hz), theta (4–7 Hz), alpha (8–12 Hz), beta (13–40 Hz) and ambient noise (59–61 Hz) frequency bands for individual analyses.

Fig. 4 superimposes the amplitude spectra for each impedance condition from a representative subject. An alpha peak at 11 Hz and a noise peak at 60 Hz are clearly identifiable. The amplitude spectra from all 5 epochs were then averaged to reduce the variance arising from temporal fluctuations brain activity. Significantly reduced alpha power can be seen in 3 trials for this subject, however, these trials were not characterized by higher electrode impedances or mismatches. In fact, there was no simple correlation between alpha power and impedance in these trials. This supports in a single subject our assertion that higher scalp-electrode impedances obtained without scalp abrasion do not result in significant signal loss in the EEG bands.

2.5. Statistical analysis

To minimize the effect of temporal fluctuations of EEG power, we restricted our statistical analyses to data averaged across subjects. Four impedance levels were defined: (1) <10 kΩ, (2) 11–20 kΩ, (3) 21–30 kΩ, and (4) 31–40 kΩ. This produced a two-factor, completely crossed, within-subject design with 16 cells: reference electrode (4 levels) × measurement electrode (4 levels). The amplitude in each frequency band was statistically analyzed using a repeated measures ANOVA, with reference and measurement channel impedance as the two within-subject factors.

3. Results

Table 1 shows the average and standard deviation (in parentheses) of the impedance values for each ANOVA cell. The first row shows the impedance ranges for the reference electrode, and the second row shows the measured values. The first column shows the impedance ranges for the measurement electrode. The last 4 rows show the impedance values for the measurement electrode, corresponding to each range for the reference electrode.

The results of the repeated measures ANOVA are discussed below for each frequency hand. In each band, the amplitude was considered first as a function of reference and measurement electrode impedance. Because 60 Hz electrical noise depends on impedance mismatch, interactions were also considered in the ANOVA.

3.1. Delta

Amplitude in the delta band did not vary significantly as a function of reference or measurement electrode impedance: $F(3, 27) < 1$ for both factors. The interaction between reference and measurement lead impedances also did not produce significant differences: $F(3, 27) < 1$.

Table 1
Scalp-electrode impedance values (kΩ) for reference and measurement electrodes

Reference	<10	11–20	21–30	31–40
	5.5 (1.9)	13.4 (1.6)	24.0 (2.6)	33.6 (2.3)
Measurement				
< 10	8.2 (1.2)	7.5 (1.2)	7.2 (1.9)	8.5 (1.1)
11–20	13.0 (2.4)	13.6 (2.6)	14.2 (2.7)	13.9 (3.0)
21–30	22.5 (2.1)	23.1 (2.7)	24.3 (3.2)	25.9 (2.5)
31–40	34.2 (2.7)	35.0 (2.7)	35.4 (3.2)	35.4 (2.9)

3.2. Theta

Amplitude in the theta band did not vary significantly as a function of reference lead impedance: $F(3,27) < 1$, or measurement lead impedance: $F(3,27) = 1.3$, $P < 0.3$. The interaction between reference and measurement lead impedances also did not produce significant differences: $F(3,27) < 1$.

3.3. Alpha

Amplitude in the alpha band did not vary significantly as a function of reference lead impedance: $F(3,27) < 1$, or measurement lead impedance: $F(3,27) = 1.2$, $P < 0.3$. The interaction between reference and measurement lead impedances also did not produce significant differences: $F(3,27) < 1$ (see Fig. 5).

3.4. Beta

Amplitude in the beta band did not vary significantly as a function of reference or measurement electrode impedance, $F(3,27) < 1$ for both factors. The interaction between reference and measurement lead impedances also did not produce significant differences: $F(3,27) < 1$.

3.5. 60 Hz Noise

Fig. 5 shows the amplitude in the 60 Hz noise and alpha bands (for comparison) as a function of scalp-electrode impedance. The amplitude in the alpha band (left) does not show a consistent trend with impedance. The amplitude in the 60 Hz noise band (right) did increase as a function of impedance, as predicted, but this effect did not reach statistical significance: $F(3,27) = 1.97, P < 0.15$ (reference lead impedance), and $F(3,27) = 1.4$, $P < 0.27$ (measurement lead impedance), or interactions: $F(3.27) < 1$ for the number of subjects and trials used here.

Fig. 6 shows the amplitude in the 60 Hz noise band as a function of impedance mismatch. The small mismatch condition was defined as the set of cases for which the reference and measurement lead impedances were in the same range (e.g. both <10 Ω). The large mismatch condition was defined as the set of all cases for which the reference and measurement lead impedances were in different and non-neighboring ranges (e.g. when one electrode impedance was <10 kΩ or 11–20 kΩ and the other electrode impedance was 31–40 kΩ. The amount of 60 Hz noise increases with the impedance mismatch, as predicted, but the increase is modest (≈8%). This suggests that only a fraction of the observed noise was due to capacitive coupling to the electrode leads. Rather, magnetic interference or other electrical mechanisms were more likely the sources of 60 Hz noise in our experiments.

4. Discussion

We have reviewed theoretically and tested experimentally the dependence of EEG signal attenuation and 60 Hz noise on scalp-electrode impedance. We have shown that if the amplifier input-impedance is high enough (≈200 MΩ), there is negligible signal attenuation when using electrodes without abrasion. This remains true even for older amplifier systems with modest input impedances (≈10 MΩ). In our experiments, using an amplifier with an input-impedance of 200 MΩ and scalp-electrode impedances up to 40 kΩ, there was no significant attenuation in any of the standard EEG frequency bands. Circuit analysis suggests that, for this input impedance, scalp-electrode impedances up to 200 kΩ still allow for accurate (≈0.1% error) signal acquisition.

Circuit analysis also showed that 60 Hz noise due to magnetic induction may be measurable, and does not depend on scalp-electrode impedance. In contrast, 60 Hz noise due to capacitive coupling to the leads increases linearly as a function of scalp-electrode impedance mismatch. This was seen visually in the data, although the effect did not reach statistical significance in this study. We therefore conclude that in our experiments most 60 Hz noise was due to magnetic fields or other electrical mechanisms.

We suggest that much of the concern over 60 Hz noise is anachronistic: a holdover from the days of paper recording in which the line noise could not be easily removed from the signal. Although 60 Hz noise is admittedly a distraction when viewing data in real time, its presence is not a practical concern for digital EEG, provided the biological signal of interest is not within 1 or 2 Hz of the 60 Hz frequency band. With accurate digital signal processing, a 60 Hz (or 50 Hz) notch filter cleanly removes this noise from the data. Earlier analog notch filters were imprecise, and were found to distort EEG features with high-frequency components, such as epileptic spikes. Although the distortion of sharp transients such as spikes should be minimal with an accurate (e.g. FIR) digital filter, the effect of each digital filtering algorithm must be verified with the EEG phenomena of interest before a high level of line noise (and thus high scalp impedance) can be tolerated. Some EEG systems currently used in clinical applications may suffer from a number of limitations, including not only much lower input impedances but also

poor values for common mode rejection ratio (CMRR) and isolation mode rejection ratio (IMRR), as well as 60 Hz notch filters with poor waveform fidelity. Furthermore, unshielded clinical equipment may introduce significantly higher noise levels. In these circumstances, it may be impossible to duplicate the results in this paper.

Skin potentials can be avoided only by puncturing the skin under the electrode (Picton et al., 2000). With modern signal analytic methods, it is unlikely that skin potentials will be confused with the coherent neural electrical fields measured with a dense sensor array. However, if avoiding skin potentials with a sparse array is desired, sterile electrodes, and not just sterile lances, must be used.

In conclusion, electrical engineering principles and experiments have demonstrated that high-quality EEG recordings can be obtained without scalp abrasion. This conclusion is not limited to the Geodesic Sensor Net or Electrical Geodesics products. It applies to any electrode design with good electrochemical and mechanical qualities, using any modern differential amplifier with an isolated grounding system and suitable capabilities for rejection of common mode noise and isolation mode noise.

Acknowledgements

The authors wish to thank Tom Renner for helpful discussions, Dennis Rech and Mary Lyda for assistance with data collection, and Mike Hartman for assistance with data analysis. This work was supported by NIH grants, R44-HL-60478, R44-AG-17399 and R44-NS-38829.

References

American Electroencephalographic Society. Report of the Committee on Infectious Diseases. J Clin Neurophysiol 1994;11:128–132.

Centers for Disease Control (CDC). (July 12, 1991). Recommendations for preventing transmission of Human Immunodeficiency Virus and Hepatitis B virus to patients during exposure-prone invasive procedures. CDC website: http://www.cdc.gov

Centers for Disease Control (CDC). (May 25, 2000). Infection control in dentistry. CDC website: http://www.cdc.gov

Ferree TC, Eriksen KJ, Tucker DM. Regional head tissue conductivity estimation for improved EEG analysis. IEEE Trans Biomed Eng 2000;47(12):1584–1592.

Gibbs CJ, Asher Jr DM, Kobrine A, Amyx HL, Sulima MP, Gajdusek DC. Transmission of Creutzfeldt–Jakob disease to a chimpanzee by electrodes contaminated during neurosurgery. J Neurol Neurosurg Psychiatry 1994;57:757–758.

Huhta JC, Webster JG. Sixty-Hertz interference in electrocardiography. IEEE Trans Biomed Eng 1973;20:91–101.

Nunez PL. Electric Fields of the Brain: The Neurophysics of EEG, Oxford University Press, 1981.

Picton TW, Bentin S, Berg P, Donchin E, Hillyard SA, Johnson Jr, R, Miller GA, Ritter W, Ruchkin DS, Rugg MD, Taylor MJ. Guidelines for using human event-related potentials to study cognition: recording standards and publication criteria. Psychophysiology 2000;37:127–152.

Putnam LE, Johnson Jr R, Roth WT. Guidelines for reducing the risk of disease transmission in the psychophysiology laboratory SPR Ad Hoc Committee on the Prevention of Disease Transmission. Psychophysiology 1992;29(2):127–141.

Rush S, Driscoll DA. EEG electrode sensitivity - an application of reciprocity. IEEE Trans Biomed Eng 1969;16(1):15–22.

Srinivasan R, Tucker DM, Murias M. Estimating the spatial nyquist of the human EEG. Behav Res Methods, Instrum Computers 1998;30:8–19.

Tucker DM. Spatial sampling of head electrical fields: the geodesic sensor net. Electroenceph clin Neurophysiol 1993;87:154–163.

Wiley JD, Webster JG. Analysis and control of the current distribution under circular dispersive electrodes. IEEE Trans Biomed Eng 1982;29(5):381–385.